Preprints.org

Article

Not peer-reviewed version

Slope Stability Assessment of Earthen Hydraulic Structures at the Dychów Pumped-Storage Power Plant Using Electrical Resistivity Tomography and Finite-Element Modelling: Implications for Ageing Critical Energy Infrastructure

Łukasz Dominik Kaczmarek * , Jacek Stasierski , Jacek Kostrzewa , Adam Lubowicki , Kacper Piekarski , Piotr Drużyński , Tadeusz Daszczyński , Maciej Filip Gruszczyński

Posted Date: 20 May 2026

doi: 10.20944/preprints202605.1349.v1

Keywords: geophysics; finite element method; earth dam; embankment; glaciotectonics

Preprints.org is a free multidisciplinary platform providing preprint service that is dedicated to making early versions of research outputs permanently available and citable. Preprints posted at Preprints.org appear in Web of Science, Crossref, Google Scholar, Scilit, Europe PMC, OpenAlex.

Copyright: This open access article is published under a Creative Commons CC BY 4.0 license, which permit the free download, distribution, and reuse, provided that the author and preprint are cited in any reuse.

Preprints.org (www.preprints.org) | NOT PEER-REVIEWED | Posted: 20 May 2026 doi:10.20944/preprints202605.1349.v1

Disclaimer/Publisher's Note: The statements, opinions, and data contained in all publications are solely those of the individual author(s) and contributor(s) and not of MDPI and/or the editor(s). MDPI and/or the editor(s) disclaim responsibility for any injury to people or property resulting from any ideas, methods, instructions, or products referred to in the content.

Article

Slope Stability Assessment of Earthen Hydraulic Structures at the Dychów Pumped-Storage Power Plant Using Electrical Resistivity Tomography and Finite-Element Modelling: Implications for Ageing Critical Energy Infrastructure

Łukasz Dominik Kaczmarek [1,*], Jacek Stasierski [1], Jacek Kostrzewa [1], Adam Lubowicki [1], Kacper Piekarski [1], Piotr Drużyński [1], Tadeusz Daszczyński [1] and Maciej Filip Gruszczyński [2]

[1] Faculty of Environmental Engineering, Warsaw University of Technology, Warsaw, Poland

[2] Faculty of Environmental Engineering and Geodesy, Wrocław University of Environmental and Life Sciences, Wroclaw, Poland

* Correspondence: lukasz.kaczmarek@pw.edu.pl

Abstract

Background: Pumped-storage hydropower (PSH) plants remain a cornerstone of grid stability and renewable-energy integration in Europe, yet a large share of the European fleet is ageing and was built under design codes that predate modern geotechnical standards. The Dychów pumped-storage power plant (ESP Dychów, 88 MW, Lubusz Voivodeship, western Poland), in service since the 1930s, is classified as part of the national critical energy infrastructure. Its earthen retaining structures have a documented history of surface mass movements – including the 1997 landslide on the frontal dam, which damaged around 60 m of the crest road and the powerhouse – and require recurrent safety assessment in complex glaciotectonic settings. **Methods:** Electrical resistivity tomography (ERT) performed in a gradient array was combined with hydrogeological observations and finite-element slope-stability analyses in ZSoil. Two cross-sections were examined – the earthen frontal dam of the upper reservoir and the embankment of the derivation channel feeding the reservoir – each with four calculation variants and two groundwater scenarios. The shear-strength reduction technique was used to obtain the "global" safety factor *SF*. **Results:** *SF* equals 1.75 for the frontal dam and ranges from 1.80 to 2.10 for the channel embankment. Parametric reduction of the internal friction angle of saturated medium sand yields limit values of φ = 12.3° (dam) and φ = 20.3° (embankment), clearly below realistic in-situ values. **Conclusions:** Both structures comply with the safety threshold F ≥ 1.50 specified for Class I hydraulic engineering structures. The presented non-invasive ERT–FEM workflow offers a cost-effective tool for the periodic reassessment of ageing PSH infrastructure, supporting its continued role in balancing variable renewable generation in decarbonising power systems.

Keywords: geophysics; finite element method; earth dam; embankment; glaciotectonics

1. Introduction

The decarbonisation of power systems across the European Union has strongly increased the demand for fast-reacting, large-scale energy storage that can complement the variable generation from wind and photovoltaic sources. Pumped-storage hydropower (PSH) is still the most mature and most widely deployed grid-scale energy-storage technology [1,2], and its role in supporting frequency control, providing reserves and enabling black-start capability is now widely recognised in the ongoing energy transition [3]. Several recent studies have addressed the flexibility of hydropower in the Polish and wider European context – including specific Polish case studies such

© 2026 by the author(s). Distributed under a Creative Commons CC BY license.

Preprints.org (www.preprints.org) | NOT PEER-REVIEWED | Posted: 20 May 2026 doi:10.20944/preprints202605.1349.v1

as the Jeziorsko reservoir on the Warta river [3,4], the evolution of Polish hydropower support schemes [5], and more broadly the development and current status of the Polish hydropower sector [6] – as well as the hydroclimatic constraints that will increasingly affect the operation of hydro schemes. What is perhaps less frequently discussed, but equally important, is that a large share of the European hydro fleet – including pumped-storage plants – is ageing and is already treated, in part, as industrial heritage [7]: many units were commissioned between the 1930s and the 1970s and were designed on the basis of codes that predate modern geotechnical standards such as Eurocode 7 [8,9]. The safe and economically attractive continuation of their operation depends, among other things, on reliable periodic assessment of the earthen retaining structures that form their civil-engineering backbone.

The Dychów hydro complex (Lubusz Voivodeship, western Poland; Figure 1) is a representative example of such an asset. It consists of seventeen hydroelectric plants located on the Bóbr, Kwisa and Nysa Łużycka rivers, with a total installed capacity of 103 MW, of which 88 MW belong to the Dychów pumped-storage power plant (hereafter ESP Dychów). The plant is the sixth-largest facility of its kind in Poland by installed capacity and is part of the national critical energy infrastructure, supporting the synchronous operation of the Polish transmission system and providing peak-shaving and ancillary services to the interconnected European grid.

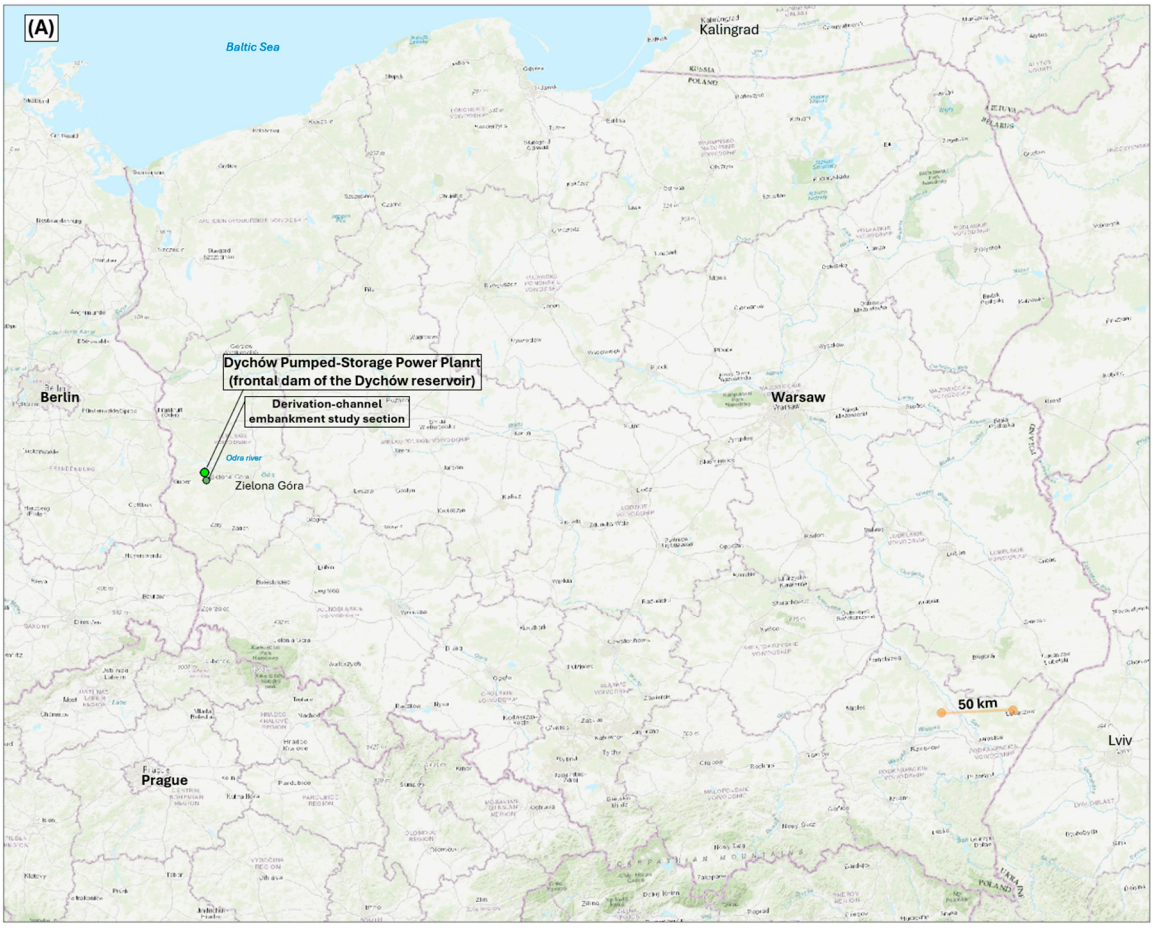

© 2026 by the author(s). Distributed under a Creative Commons CC BY license.

Preprints.org (www.preprints.org) | NOT PEER-REVIEWED | Posted: 20 May 2026 doi:10.20944/preprints202605.1349.v1

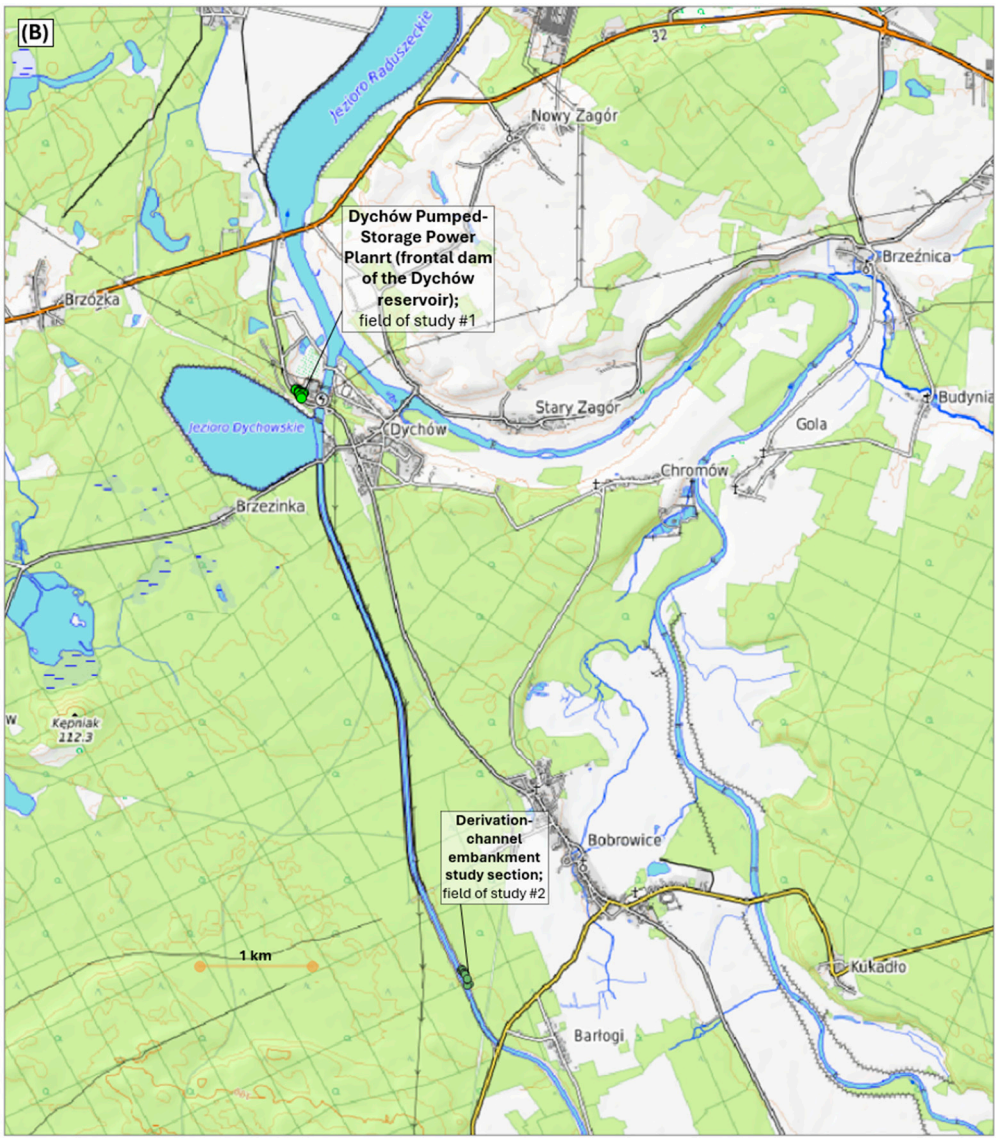

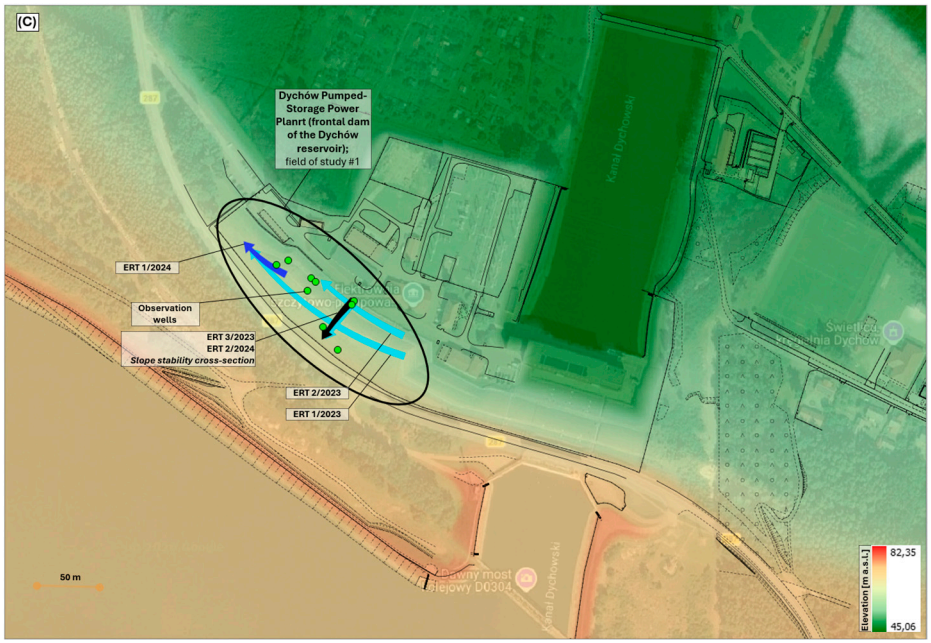

© 2026 by the author(s). Distributed under a Creative Commons CC BY license.

Preprints.org (www.preprints.org) | NOT PEER-REVIEWED | Posted: 20 May 2026 doi:10.20944/preprints202605.1349.v1

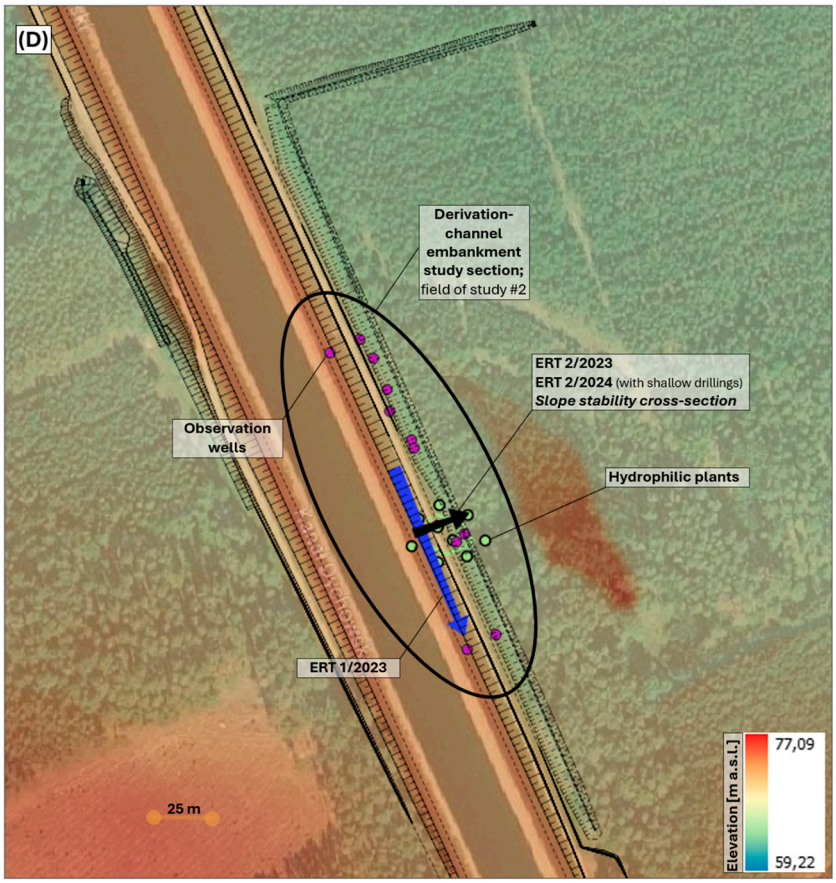

Figure 1. Fields of study: (A) location regional map (based on ESRI topography map); (B) location local map (based on OSM topography); (C) Dychów Pumped-Storage Power Plant (frontal dam of the Dychów reservoir); (D) Derivation-channel embankment study section.

The Dychów plant was built between 1932 and 1936 and, after numerous modernisations, is still in operation. Its ninety-year history has brought several challenges, both in terms of technical maintenance and of safety of the earthen structures, the latter resulting from difficult subsoil and groundwater conditions [10]. In 1997 a dangerous surface mass movement took place on the frontal dam of the upper reservoir. The landslide was probably a consequence of long-lasting rearrangement of the soil skeleton within the dam body, caused by intensive and prolonged filtration. It destroyed about 60 m of the crest road and caused significant damage to the powerhouse building [11], with a direct impact on plant availability. Excessive seepage from the upper reservoir resulted from a marked deterioration of the bottom and upstream-face sealing in the dam area, combined with complex ground conditions in the foundation layer – in particular the naturally unfavourable, inclined contacts of soil layers disturbed by glaciotectonics. The top of the cohesive clays interbedded with till and non-cohesive sands and gravels, lying at the base of the slope, formed a preferential pathway both for groundwater flow and for moving landslide masses. Events of this kind underline that, from the point of view of the electric-power system, the reliability of a PSH unit depends not only on the electromechanical equipment but, to a large extent, also on the condition of the civil structures that impound the upper reservoir and convey the water.

The study addresses the stability of selected earthen slopes of the hydraulic structures of the Dychów plant, identified as particularly prone to damage or failure. The areas of interest and the calculation cross-sections were chosen on the basis of field reconnaissance and consultations with the technical staff responsible for the operation and maintenance of the plant. A cross-section of the earthen frontal dam was prepared and analysed with regard to the previously documented seepage, suspicions of body soils loosening process. A second cross-section was developed for the stability analysis of the downstream slope of the embankment of the derivation channel that feeds the upper

© 2026 by the author(s). Distributed under a Creative Commons CC BY license.

Preprints.org (www.preprints.org) | NOT PEER-REVIEWED | Posted: 20 May 2026 doi:10.20944/preprints202605.1349.v1

reservoir, within a reach where an intensive, above-average growth of hydrophilic vegetation is systematically observed. The channel embankment crosses a natural depression whose morphology suggests risk of surface runoff.

Slope stability was analysed for a set of variants covering different boundary conditions, both hydrogeological settings and the strength characteristics of the soils that form the structures and their subsoil. Numerical models were defined on the basis of the relevant geological-engineering literature, the ERT results and supplementary hydrogeological observations.

The stability of the selected earthen retaining structures was analysed with regard to the recommendations of the Regulation of the Minister of Environment of 20 April 2007 on the technical conditions to be met by hydraulic structures and their location [12]. The analysis also took into account the most frequent causes of slope instability in Poland reported in the literature [13]: loading by buildings or embankments (30.8% of landslides), erosional undercutting (23.1%), infiltration of rainwater (20.0%), design errors (10.8%), undercutting by excavation (10.8%) and abrasion (4.5%).

The scope of the work covered the analysis of available archival materials and of the domestic and international subject literature. On this basis, the site conditions and the structures of interest were described. Next, the geophysical data (geoelectric cross-sections) were analysed together with a reinterpretation of the archival documentation. Hydrogeological measurements were then used to produce maps of the groundwater-table elevation (hydroisohypses). Both the hydrogeological maps and the spatial integration of data were prepared within a dedicated geographic information system (Quantum GIS). In this way, conceptual numerical models of the ground were established and used in the stability analyses aimed at determining the "global" safety factor *SF*. The calculations were performed with ZSoil, a specialised finite-element package implementing the shear-strength reduction method. The results, expressed both quantitatively and qualitatively, are summarised in the final part of the paper.

The main contribution of this paper is not a new geophysical or numerical method, but a repeatable assessment procedure assembled from existing tools and adapted to ageing pumped-storage structures of critical energy-infrastructure rank. The procedure couples a fixed-profile ERT survey, repeated in defined period (i.e. every one or two years) and co-registered with GNSS, with a hydrogeological reinterpretation and a finite-element shear-strength-reduction model. Because the profiles keep the same position and are located with GNSS, the cross-sections obtained in different years can be compared, so the same workflow gives at once the current factor of safety and a first indication of slow changes in the soil structure, without any permanent instrumentation of the dam or the embankment. For this reason the procedure can be applied, at a comparable cost, to a larger group of Class I hydraulic structures of an ageing hydropower fleet, and not only to a single object. The Dychów plant is used here as a worked example of such a periodic reassessment.

2. Geological and Engineering Conditions of the Study Area

Two objects of the Dychów pumped-storage plant, both located in the Bobrowice region, are the subject of this study: the earthen frontal dam of the upper reservoir, and the embankment of the derivation channel connecting the Bóbr river to the Dychów reservoir.

The main parameters of the frontal dam are as follows: height 27 m, crest width 11.25 m, crest length 573 m. The upstream-slope inclination is 1:2.5 to 1:3, and the downstream slope 1:2.

The Dychów channel is an artificial derivation channel running between the villages of Krzywaniec and Dychów. Its length is 20 km, width 20 m and depth about 8 m. The cross-section has a trapezoidal shape; the banks and bottom are protected with reinforced-concrete slabs, forming a barrier that separates the channel water from the groundwater. The channel supplies water to Lake Dychów and is also a local tourist attraction.

Based on the analysis of archival materials [14] and of the detailed geological maps of the surface [15–18], complex ground conditions can be stated for the area of interest with regard to glaciotectonics. Partially complex conditions also occur in those reaches of the embankment where the top of the glaciotectonically disturbed deposits lies below the embankment base.

© 2026 by the author(s). Distributed under a Creative Commons CC BY license.

Preprints.org (www.preprints.org) | NOT PEER-REVIEWED | Posted: 20 May 2026 doi:10.20944/preprints202605.1349.v1

In the area of the frontal dam (Figure 2), made-up sand fills occur (with an average thickness of about 10 m), resting on sandy tills of considerable thickness (up to several tens of metres) with an irregular top surface. These conditions are responsible for groundwater damming in the upper part of the dam, which translates into an increased hydraulic gradient and a risk of developing internal erosion, as well as an increase in the plasticity index of the cohesive soils.

In the analysed reach of the channel embankment (Figure 3), the ground is more homogeneous. From the ground surface downwards, the profile consists of made-up medium sands, followed by clayey sands, saturated sands, and sandy tills.

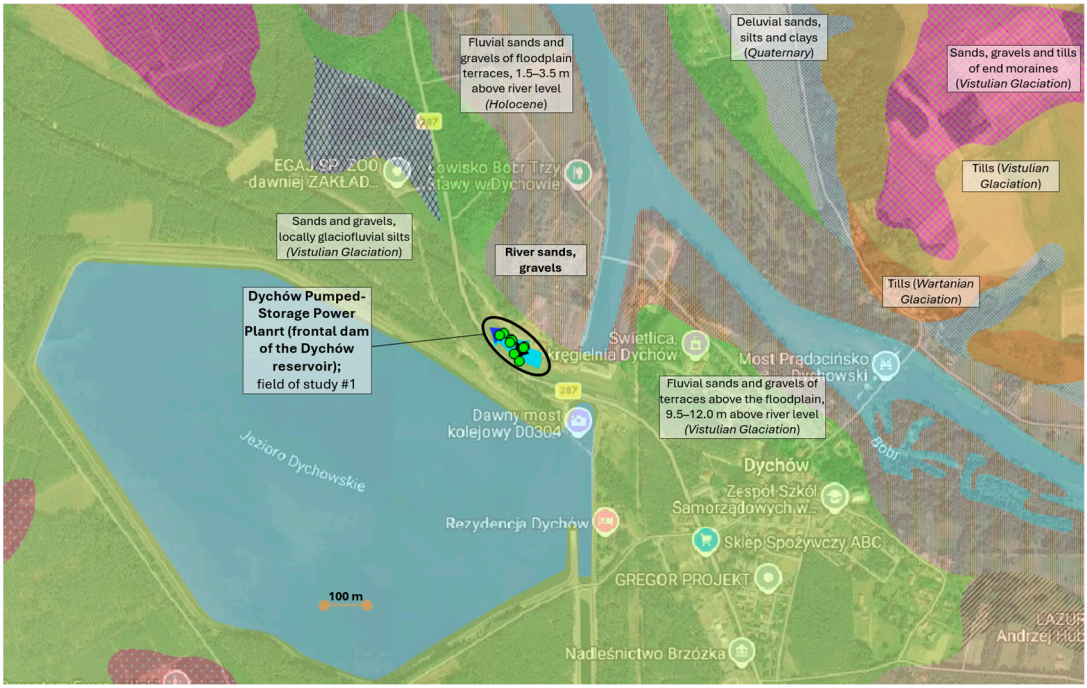

Figure 2. The location of the investigations on the the frontal dam of the Dychów reservoir with detailed geological map of Poland in the background [15].

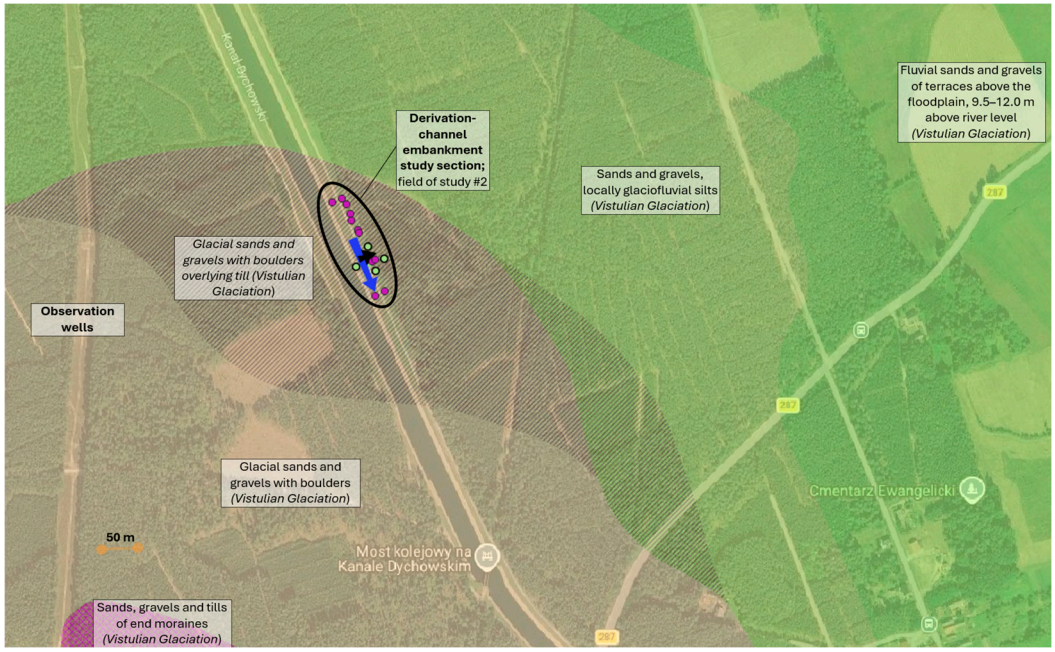

Figure 3. The location of the investigations on the derivation-channel embankment with detailed geological map of Poland in the background [15].

© 2026 by the author(s). Distributed under a Creative Commons CC BY license.

Preprints.org (www.preprints.org) | NOT PEER-REVIEWED | Posted: 20 May 2026 doi:10.20944/preprints202605.1349.v1

3. Methods

Following the provisions of Eurocode 7 (PN-EN 1997) [8,9], concerning geotechnics, and the calculation procedures used for the assessment of earthen and foundation structures, the analyses were based on advanced computational techniques employing the finite element method (FEM). This method allows a precise reproduction of complex ground conditions and of the geometry of the analysed objects (the dam and the embankment). In the context of hydraulic structures, the shear-strength reduction (SRM) technique implemented within FEM codes [19,20] has been successfully applied for the slope stability evaluation of dam foundations under seepage and hydraulic–mechanical coupling.

The following procedure was applied in order to determine the safety factor:

(1) Field reconnaissance (periodic, 2 years period) with hydrogeological observations (groundwater table, ER, TDS, temp.; 09.2023 and 09.2024; air temperature above 20°C), GNSS measurements, shallow boreholes.

(2) The digital terrain model was used to define the calculation profiles of the ground surface. The source data were obtained from airborne laser scanning, distributed by the Head Office of Geodesy and Cartography in Warsaw.

(3) Based on the results of the geophysical surveys (electrical resistivity tomography, ERT) [21], the division of the model into material zones (soil layers) was defined. The ERT profiles were measured in a gradient array; the electrode spacing and the resolution were adapted to each profile, and their lengths, maximum prospection depths and inversion errors are collected in Table 1. During post-processing a topographic correction was applied. The ERT investigations were repeated twice, year by year (in 2023 and 2024; thanks to the GNSS measurements), along the same profiles. The comparison of the prospection results gives information about potential changes of the soil structure. Details of the ERT prospection are given in Table 1.

(4) The model was supplemented with boundary conditions describing the position of the groundwater table. Piezometric observations, the hydrogeological map of Poland and a dedicated own hydroisohypse map were used for this purpose (generated in QGIS, using the multilevel B-spline interpolation from the SAGA toolset [22]).

(5) Finite-element discretisation schemes were prepared, and material properties were assigned to the corresponding zones. For the models, the factor of safety was calculated with the shear-strength reduction method (c–φ reduction) implemented in ZSoil.

Table 1. ERT prospection methodological information.

Location	*Profile*	Profile length (m)	Max. prospection depth (m)	Electrode spacing (m)	Approximation (inversion) error (RMS)
Dam (field study #1)	***ERT 1/2023***	160	~35	2	9.8 % (iter. 7)
	ERT 2/2023	80	~17	1	3.1 % (iter. 5)
	ERT 3/2023	40	~10	1	1.5 % (iter. 7)
	ERT 1/2024	40	~9	0.5	3.4 % (iter. 6)
	ERT 2/2024	40	~9	0.5	2.5 % (iter. 7)
Embankment (field study #2)	***ERT 1/2023***	80	~16.5	1	2.2 % (iter. 7)
	ERT 2/2023	28	~5	0.5	0.91 % (iter. 7)

The successive stages of the calculations included: (i) the determination of the safety factor for the model reproducing the actual ground and water conditions; (ii) the determination of the safety factor for other possible variants of soil state and strength parameters; and (iii) the identification of

© 2026 by the author(s). Distributed under a Creative Commons CC BY license.

Preprints.org (www.preprints.org) | NOT PEER-REVIEWED | Posted: 20 May 2026 doi:10.20944/preprints202605.1349.v1

the limit value of the internal friction angle of the sands at which the safety factor reaches 1.00 (e.g., as a consequence of a strength loss associated with internal erosion).

4. Geophysical Survey Results

The results of the geophysical surveys (ERT) are presented below as resistivity cross-sections, obtained on the frontal dam of the Dychów reservoir (Figure 4) and on the derivation-channel embankment (Figure 5).

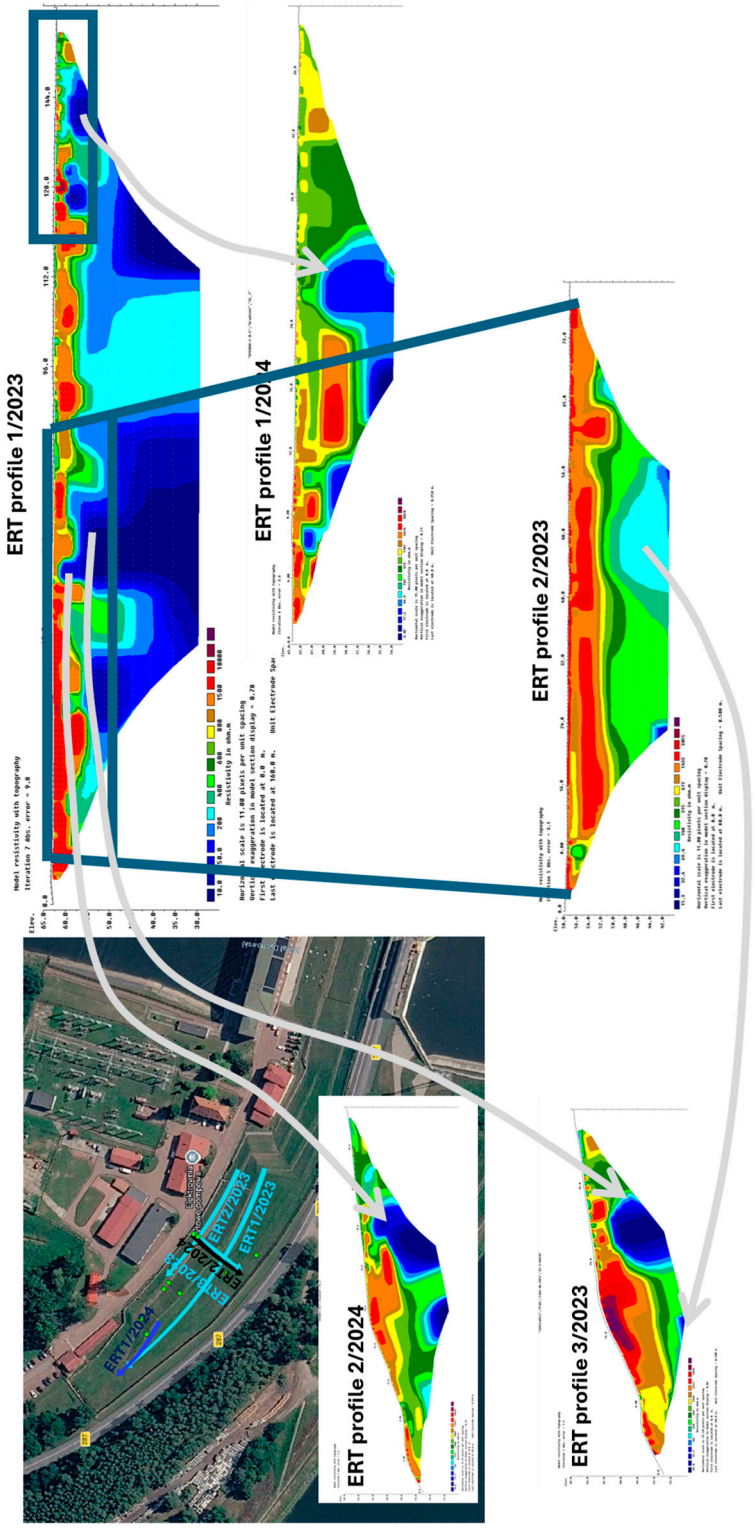

Figure 4. Resistivity cross-section of the profile measured on the frontal dam of the Dychów reservoir.

© 2026 by the author(s). Distributed under a Creative Commons CC BY license.

Preprints.org (www.preprints.org) | NOT PEER-REVIEWED | Posted: 20 May 2026 doi:10.20944/preprints202605.1349.v1

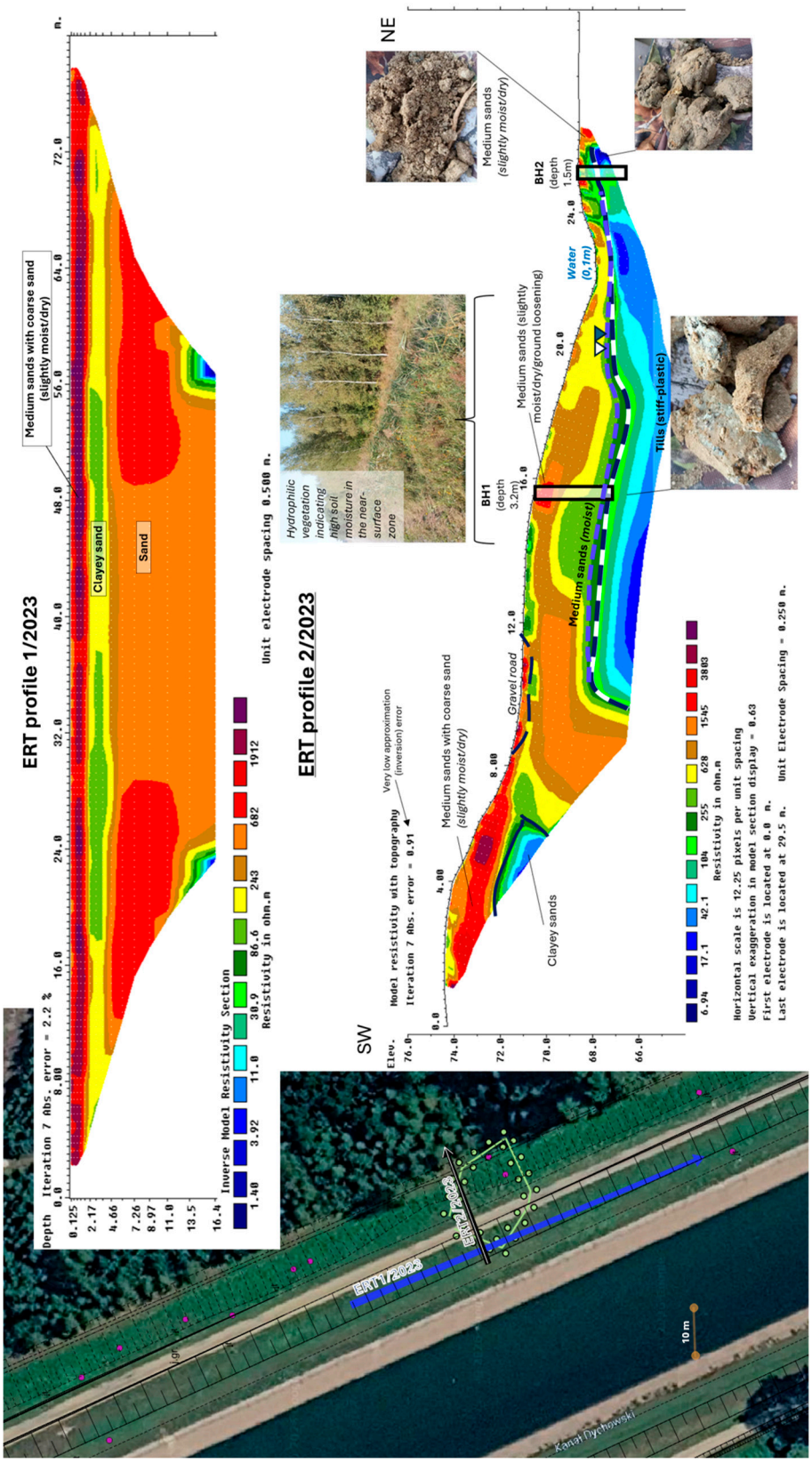

Figure 5. Resistivity cross-section of the profile measured on the derivation-channel embankment.

The colour scale represents resistivity values, which mainly reflect lithology, then the saturation of the pore space and the porosity. In both cross-sections, zones of low resistivity (below about 80 Ωm) and of high resistivity (above about 500 Ωm) can be identified. The former correspond to cohesive soils (blue and green), while the latter correspond to soils dominated by the sand fraction

© 2026 by the author(s). Distributed under a Creative Commons CC BY license.

Preprints.org (www.preprints.org) | NOT PEER-REVIEWED | Posted: 20 May 2026 doi:10.20944/preprints202605.1349.v1

(dark red and brown). The intermediate zones (80–500 Ωm) are associated with a larger content of silt or clay fractions, or with the presence of groundwater (yellow and orange).

In the area of the frontal dam, the top of the cohesive soils is strongly disturbed, which is related to the glaciotectonic history of the area. A similar observation holds for the derivation channel, where the top of the cohesive soils is not flat-parallel either; in the longitudinal geophysical profile taken along the embankment crest, this zone drops below the base of the embankment body.

On the basis of the geological background, an interpretation was performed whose results – were reproduced within the models implemented in ZSoil (Figures 6 and 7).

The calculation cross-section of the dam extends over a length of 120 m, encompassing the zone identified as potentially initiating mass movements that could lead to loss of stability (a steep slope combined with a local rise of the cohesive soils, sandy tills, whose top surface forms a potential preferential slip zone). In the second case, the stability analysis was restricted to the zone where the glaciotectonic disturbances appear at shallow depth.

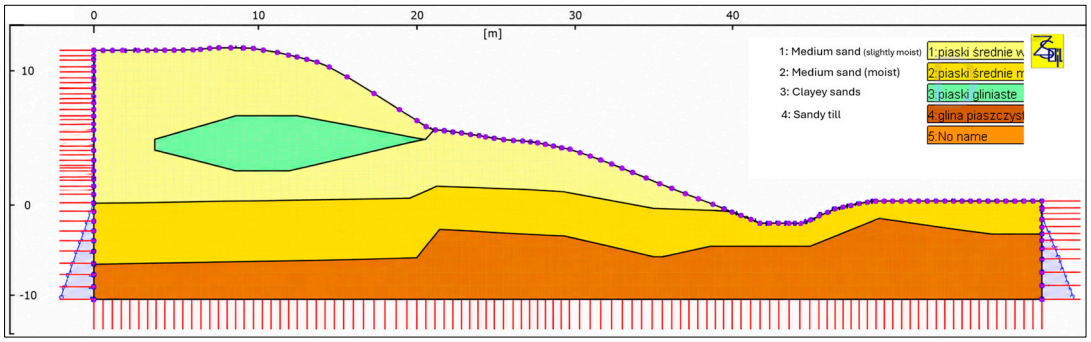

Figure 6. Cross-section of the frontal dam with soil layers and ground-surface elevations.

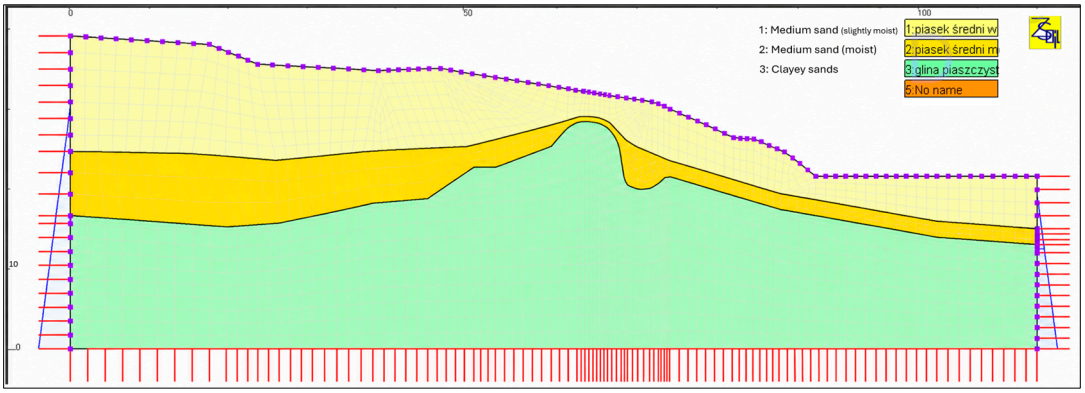

Figure 7. Cross-section of the derivation-channel embankment with soil layers and ground-surface elevations.

5. Calculation Variants and Soil Parameters

The variants and calculation assumptions adopted in the ZSoil models of the dam and the embankment are listed below:

Variant 1 – soil layers from the ground surface downwards: moist medium sand; saturated medium sand; hard-plastic sandy till.

Variant 2 – soil layers from the ground surface downwards: moist medium sand; saturated medium sand, with a reduced internal friction angle corresponding to F = 1.00; hard-plastic sandy till.

Variant 3 – soil layers from the ground surface downwards: moist medium sand; saturated medium sand; plastic sandy till (about 1 m thick top layer); then hard-plastic sandy till.

© 2026 by the author(s). Distributed under a Creative Commons CC BY license.

Preprints.org (www.preprints.org) | NOT PEER-REVIEWED | Posted: 20 May 2026 doi:10.20944/preprints202605.1349.v1

Variant 4 – soil layers from the ground surface downwards: moist medium sand; saturated medium sand, with a reduced internal friction angle corresponding to F = 1.00; plastic sandy till (about 1 m thick top layer); then hard-plastic sandy till.

The position of the groundwater table for variants 1–4 (Table 2) was defined on the basis of field piezometric measurements (scenario A) and on the hydroisohypse pattern presented in the hydrogeological map of Poland [16,17] (scenario B).

Table 2. Groundwater-table elevations adopted as hydrostatic boundary conditions in the calculation variants of the numerical models (m a.s.l.).

Variant	Frontal dam		Channel embankment	
	Left edge	Right edge	Left edge	Right edge
Field measurements (A)	61.60	50.26	68.91	68.20
Hydrogeological map (B)	60.00	50.00	69.50	68.00

On the basis of these elevations, the risk of static liquefaction of the sands present within the cross-sections was checked. The calculations showed a wide safety margin with respect to static liquefaction. However, this does not eliminate the risk associated with sudden and unfavourable weather conditions, or with accidental situations related to leakage from the reservoir or the derivation channel.

In variants 2 and 4 automated parametric calculations were performed, consisting of a step-wise reduction of the internal friction angle φ of the saturated medium sand until the limit value was reached. The reduction step was 1°, and the factor of safety was determined with an accuracy of 0.05.

The soil parameters (Table 3) adopted for the calculations (moist medium sand, saturated medium sand, clayey sand, hard-plastic sandy till and plastic sandy till) were estimated on the basis of the regional literature [23,24], consistent with archival materials and the geological cross-sections. An ideally elastic–perfectly plastic model with the Mohr–Coulomb failure criterion was assumed for all soil layers.

Table 3. Summary of soil parameters adopted in the numerical stability analyses.

Soil parameter	Medium sand (moist)	Medium sand (saturated)	Clayey sand	Sandy till (hard-plastic)	Sandy till (plastic)
Deformation modulus, E (MPa)	87.0	87.0	20.6	38.6	24.6
Poisson's ratio, ν (–)	0.25	0.25	0.30	0.25	0.25
Specific gravity, γ_s (kN/m³)	26.5	26.5	26.5	26.7	26.7
Bulk unit weight, γ (kN/m³)	18.5	20.0	21.5	21.5	20.5
Natural water content, w_n (%)	14.0	22.0	13.0	16.0	21.0
Hydraulic conductivity, k (m/d)	$1.2 \cdot 10^{-1}$	$1.2 \cdot 10^{-1}$	$1.2 \cdot 10^{-4}$	$1.2 \cdot 10^{-4}$	$1.2 \cdot 10^{-4}$
Cohesion, c (kPa)	0.0	0.0	17.0	39.3	31.3
Internal friction angle, φ (°)	33.3	33.3	14.8	21.5	18.1

© 2026 by the author(s). Distributed under a Creative Commons CC BY license.

Preprints.org (www.preprints.org) | NOT PEER-REVIEWED | Posted: 20 May 2026 doi:10.20944/preprints202605.1349.v1

Dilatancy angle, ψ (°)	3.30	3.30	1.85	2.70	2.30
Earth-pressure coefficient at rest, K_0 (–)	0.45	0.45	0.75	0.63	0.69
Relative density, I_D (–)	0.55	0.55	–	–	–
Liquidity index, I_L (–)	–	–	0.20	0.20	0.40

6. Stability Analysis Results

The results of the stability calculations were examined both quantitatively (by listing the obtained factors of safety) and qualitatively (by considering the location, extent and shape of the potential slip surfaces bounding the possible surface mass movements). Within the calculation variants, the possible states of the top layer of sandy till and the influence of different values of the internal friction angle of the saturated medium sand on the factor safety were examined. Both the quantitative results and their qualitative analysis made it possible to assess the safety margin with respect to the activation of potential landslides and to identify the most vulnerable areas.

6.1. Frontal Dam of the Dychów Pumped-Storage Power Plant

The position of the groundwater table for variants 1–4 in the analysed cross-section of the frontal dam is shown in Figure 8. The differences are very small between scenario A and B (Table 2).

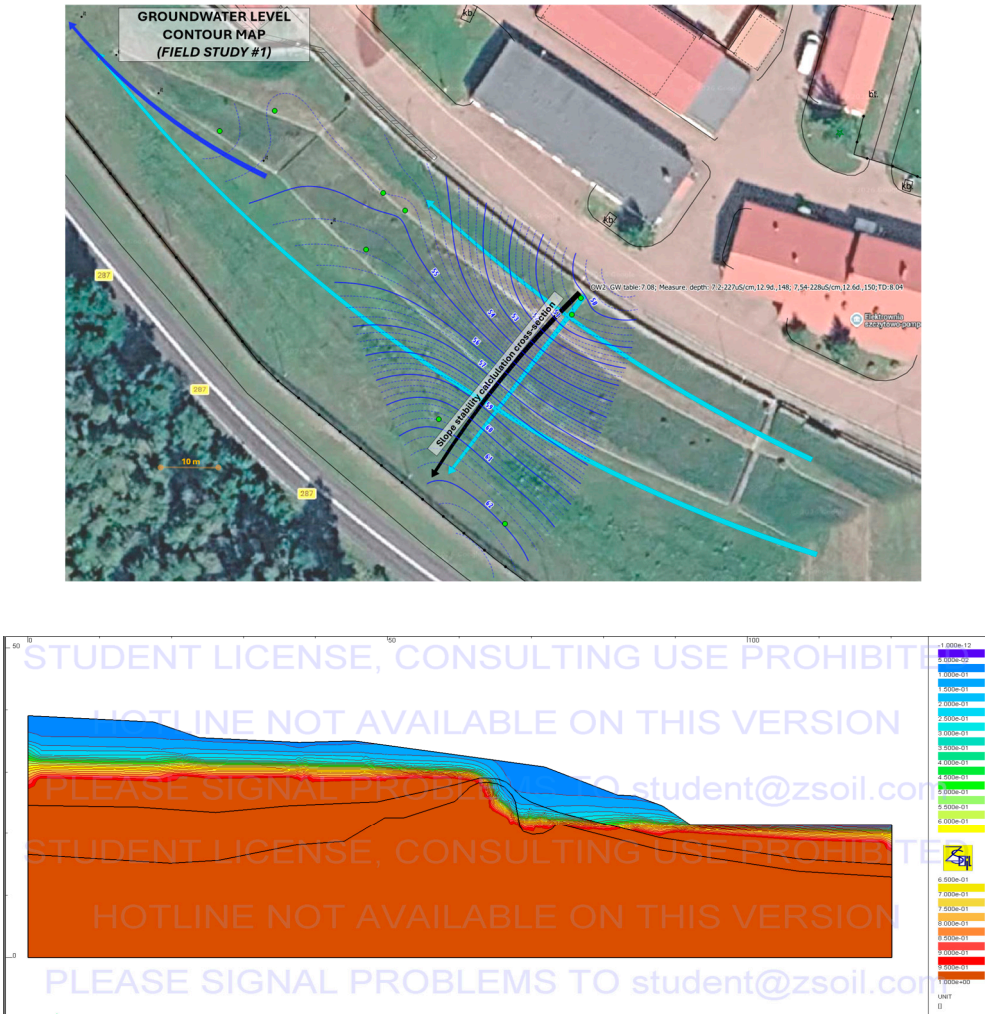

Figure 8. Degree of water saturation of the subsoil of the frontal dam (brown indicates soil below the groundwater table; full saturation): scenario A (a slightly higher hydraulic gradient than in scenario B).

© 2026 by the author(s). Distributed under a Creative Commons CC BY license.

Preprints.org (www.preprints.org) | NOT PEER-REVIEWED | Posted: 20 May 2026 doi:10.20944/preprints202605.1349.v1

In the first case (scenario A, Figure 8), the groundwater table adopted in the model was documented by observations in open piezometers. At the location of the largest glaciotectonic disturbance, a significant difference in groundwater levels is visible. Such a situation impedes groundwater flow and, during intense rainfall, may lead to a sudden increase in filtration under a high hydraulic gradient. As a consequence, a temporary internal erosion could be initiated, which might in turn loosen the non-cohesive soil skeleton. Confirming such a scenario would require longer and more detailed observations of the groundwater table as well as granulometric analyses of the soils.

The second case (scenario B) differs from the first (scenario A, in that the groundwater table is lower by 1.6 m at the left edge of the model, with a proportional reduction of the hydraulic gradient. This scenario corresponds to the documented hydroisohypse pattern presented in the hydrogeological map of Poland. The resulting lowering of the groundwater level is not expected to have a negative impact on the safety of the dam with respect to landslide hazard. The stability calculations showed that the 1.6 m lowering of the groundwater table at the left edge of the model has practically no influence on SF or on the shape of the slip surface; the only effect was a reduction of the limit internal friction angle of the sands by about 1°.

The potential slip surfaces on the frontal dam, for the different variants of soil parameters (1–4) and groundwater positions (A, B), are shown in Figure 9.

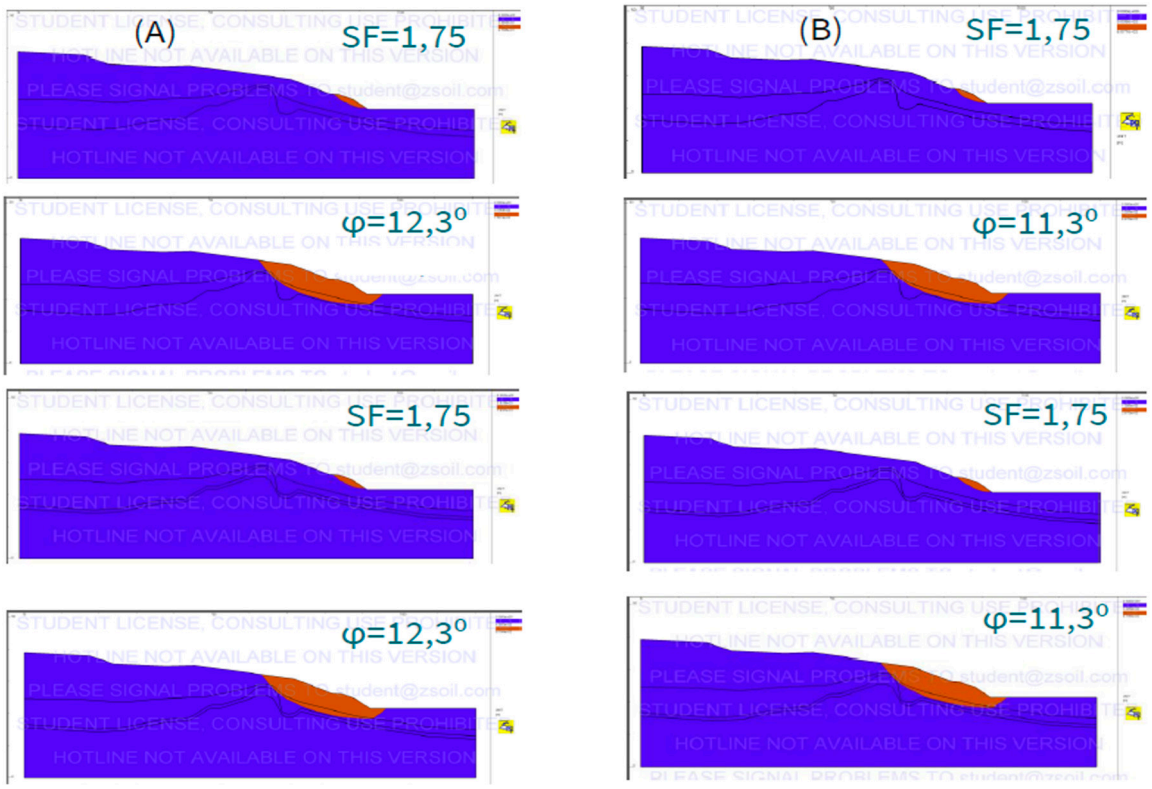

Figure 9. Potential slip surfaces of the hypothetical landslide on the frontal dam: scenario A – groundwater position based on field measurements; scenario B – groundwater position based on the hydroisohypse pattern from the hydrogeological map of Poland.

In variant 1A the factor of safety equals 1.75. No significant influence of groundwater is observed, which is related to the location of the potential landslide. The calculations indicate a near-surface zone (with a shape close to a slide, Figure 9, 1A) as the hypothetical zone of deformation development, lying entirely above the groundwater table (Figure 8a). The main destabilising factor is the inclination of the lower part of the downstream slope of the frontal dam. The slip surface is about 10 m long, covering only the steepest portion of the lower slope and a layer of moist medium sand no more than a few metres deep.

© 2026 by the author(s). Distributed under a Creative Commons CC BY license.

Preprints.org (www.preprints.org) | NOT PEER-REVIEWED | Posted: 20 May 2026 doi:10.20944/preprints202605.1349.v1

In variant 2A (Figure 9, 2A), the safety factor SF ≈ 1 for the downstream slope of the frontal dam was obtained through step-wise reduction of the internal friction angle of the saturated medium sand down to $\varphi = 12.3°$. With the groundwater table included in the model, the limit value still corresponds to F ≈ 1 – no "visible" (calculation step ΔSF = 0.05) changes here, because the glaciotectonic impermeable tills uphill have an impact. The computed slip surfaces, regardless of the case, are very similar and take a circular–cylindrical shape. The extent of the theoretical landslide in this variant is about 32 m between the extreme points of the slip surface. This is larger than in variant 1A, and covers a wider part of the slope. In terms of depth, the slip surface reaches into the moist and saturated medium sand layers (the depth of the hypothetical landslide reaches about from several to ten metres). In this case, the slip surface rests on the top of the cohesive soils (hard-plastic sandy till) that underlie the sands, which shows a significant influence of the state of this till, especially in the top zone, on the extent of the potential landslide.

Variants 3A and 4A differ from variants 1A and 2A by the presence of a layer of plastic sandy till in the top zone of the underlying hard-plastic moraine till. For variant 3A, because the computed slip surface lies close to the ground surface, changes of the soil state at greater depth did not cause any noticeable change either in the factor of safety or in the geometry of the slip curve (Figure 9, 3A). For variant 4A (Figure 9, 4A), the limit value $\varphi = 12.3°$ was again obtained for SF ≈ 1; the mobilised soil masses again consisted mainly of sands resting on the till. It can therefore be stated that a reduction of cohesion and internal friction angle by approximately 20% (Table 3), corresponding to a simulated change of the till state from hard-plastic to plastic, is not significant and does not produce noticeable qualitative differences with respect to variants 1A and 2A.

The results for variant 1B are identical to those of variant 1A (SF = 1.75, and the slip surface is in the same position). In this case, as well as in variant 3B (SF = 1.75), no influence of the changes in the calculation scheme on the stability was observed. This is due to the clear dominance of a potential slip surface located in the near-surface zone and to the lack of direct interaction between groundwater and this part of the structure.

In the remaining variants (2B and 4B) the slip surfaces lie below the groundwater table. Consequently, lowering of the groundwater level led to an even larger safety margin, expressed by a limit value $\varphi = 11.3°$ (for SF ≈ 1).

6.2. Derivation-Channel Embankment

The position of the groundwater table for variants 1–4 in the analysed cross-section of the derivation-channel embankment is shown in Figures 10a (scenario A) and 10b (scenario B).

As in the case of the frontal dam, the documented groundwater table in the analysed cross-section of the channel embankment lies below the base of the embankment.

The saturation boundary in scenario A (Figure 10a) has a small gradient (the difference in pressure head between the model edges equals 0.7 m), and a well-functioning drain is located at the foot of the embankment slope. Figure 10a shows the depression curve for scenario A (variants 1–4).

In the second calculation scenario (B) the hydraulic gradient was increased (the difference in pressure head between the side edges of the model was raised from 0.7 m to 1.5 m). Figure 10b shows the groundwater-table position for scenario B (variants 1–4).

The potential slip surfaces in the channel embankment, for the different variants of material parameters (1–4) and groundwater positions (A, B), are presented in Figure 11.

In the case without groundwater, with a shallow slip surface, the factor of safety does not change (Figure 11, 1A). The landslide strip is about 6 m wide and would be located in the upper part of the slope, covering only the layer of moist medium sand.

© 2026 by the author(s). Distributed under a Creative Commons CC BY license.

Preprints.org (www.preprints.org) | NOT PEER-REVIEWED | Posted: 20 May 2026 doi:10.20944/preprints202605.1349.v1

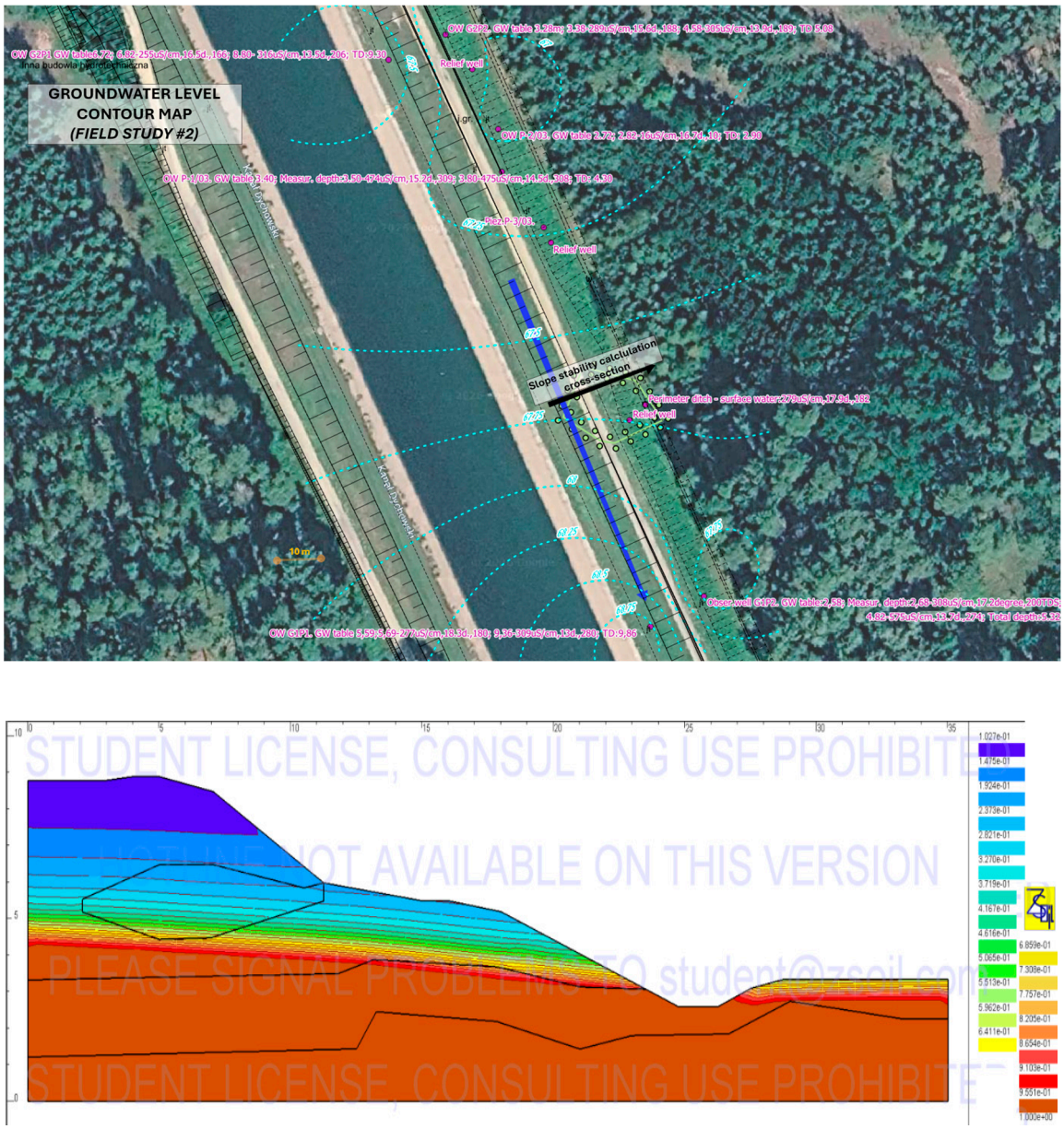

Figure 10. Degree of water saturation of the subsoil of the embankment slope (brown indicates soil below the groundwater table; full saturation): scenario B (a slightly higher hydraulic gradient than in scenario A).

Under realistic conditions, i.e. with groundwater present – even below the base of the embankment (Figure 11, 1A) – the safety level of the analysed slope varied depending on the assumptions of each variant.

In variant 1A the factor of safety decreased slightly, to a value of 2.0. The extent of the landsliding processes also changed: two potential landslides may develop (Figure 11, 1A). The first one, as in the case without groundwater, is located in the upper part of the body. The second one, in the lower part, is about 8 m wide and involves the layer of saturated medium sand. Both slide bodies are of surface-mass-movement type, with a depth not exceeding a few metres. Although the "global" safety factors are similar, the potential landslide in the lower part of the slope should be considered more prone to activation. This is mainly due to the presence of the nearby service road designed for heavy vehicles, which may act as an additional destabilising factor of dynamic character directly affecting this lower part of the body (Figure 11, 1A). It should be noted that for such shallow and relatively short slip surfaces, dynamic loading from heavy traffic may change the ratio between driving and resisting forces considerably more than for long and deep slip surfaces; therefore, in a more detailed design-level analysis, an additional road load should be applied to the slope in accordance with the road-

© 2026 by the author(s). Distributed under a Creative Commons CC BY license.

Preprints.org (www.preprints.org) | NOT PEER-REVIEWED | Posted: 20 May 2026 doi:10.20944/preprints202605.1349.v1

engineering standard. Nevertheless, the obtained safety factor (2.0) still indicates a considerable reserve of capacity.

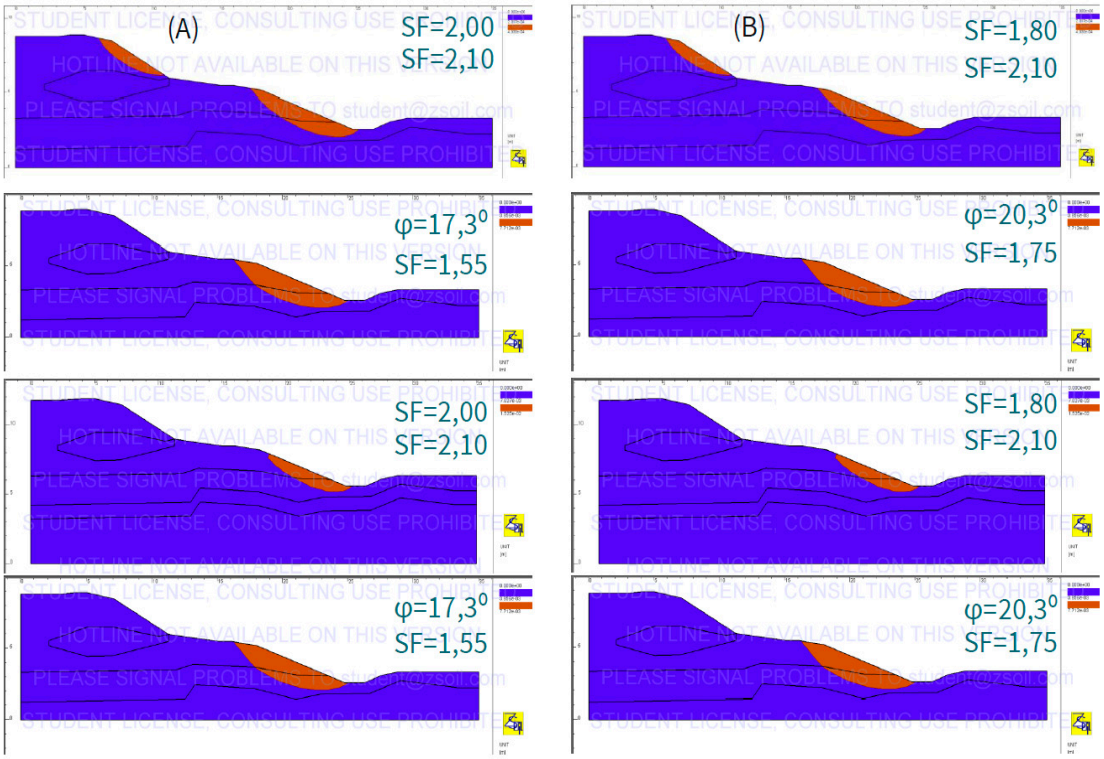

Figure 11. Potential slip surfaces of the hypothetical landslide on the embankment slope: scenario A – groundwater position based on field measurements; scenario B – groundwater position based on the hydroisohypse pattern from the hydrogeological map of Poland.

In the parametric analysis (variant 2A), in which the internal friction angle of the saturated medium sand was gradually reduced to reach the limit value SF = 1.00, a limit angle φ = 17.3° was obtained. This limit value corresponds to the case with groundwater included in the model.

When the groundwater is removed from the model while keeping φ = 17.3°, the safety factor rises to 1.55, consistently with the fact that, in non-cohesive soils, the presence of water reduces the overall shear capacity of the slope. The slip surfaces in variant 2A are located similarly to those in the previously described variants. However, both with and without groundwater, a single slip surface is obtained in the lower part of the slope (Figure 11, 2A). This surface cuts off a wedge about 8 m wide and no more than a few metres deep. This results from the degradation of the strength parameters of the saturated medium sand in the lower part of the slope.

The following variants (3A and 4A) may illustrate the consequences of long-term groundwater action on the top of the moraine hard-plastic sandy till (Figure 11, 3A–4A). The top zone was modelled here as a layer of plastic sandy till. The calculations yielded factors of safety consistent with those of variants 1A and 2A, which can be explained by the location of the potential slip surfaces above the top of the hard-plastic and plastic till layers. Despite the weakening introduced in the top of the till, no lowering of the slip surfaces – and therefore no deepening of the landslides – is observed. Although the factors of safety are similar, the qualitative assessment of variants 3A and 1A reveals meaningful differences. Without groundwater, the upper part of the body is more endangered, whereas with groundwater the lower part is (Figure 11, 3A–4A). In variant 4A the qualitative pattern remains the same as in variant 2A (only one slip surface in the lower part of the embankment).

Changes in the saturated zone in the model of the channel embankment for variants 1B and 3B led to quantitative changes of the results with respect to, respectively, variants 1A and 3A. In variants

© 2026 by the author(s). Distributed under a Creative Commons CC BY license.

Preprints.org (www.preprints.org) | NOT PEER-REVIEWED | Posted: 20 May 2026 doi:10.20944/preprints202605.1349.v1

1B and 3B the factor of safety with groundwater present decreased from 2.00 to 1.80, while without groundwater it remained the same (2.10).

Similar relationships were found for the remaining B variants compared with the first group (A variants). Despite the quantitative differences, no significant qualitative changes were observed. In variants 2B and 4B, the step-wise reduction of the internal friction angle of the saturated medium sand led to a limit value $\varphi = 20.3°$ (at SF = 1.00). Without groundwater, the factor of safety with $\varphi = 20.3°$ equals 1.75.

7. Discussion

The results show that, despite the complex glaciotectonic history of the cohesive soils in the area, both analysed structures preserve a safety factor well above the required value SF = 1.50 [12]. For the frontal dam, SF = 1.75 in all considered variants, and for the channel embankment the values range from 1.80 to 2.10. This is in line with the general observation that ageing earthen hydraulic structures built on glacial and glaciotectonically disturbed subsoil in western Poland may still offer a sufficient safety reserve, provided that seepage control and drainage remain functional [10,13].

Parametric reduction of the internal friction angle of the saturated medium sand provided useful information on the robustness of the structures with respect to progressive weakening of the non-cohesive body soils. The limit values $\varphi = 12.3°$ (dam) and $\varphi = 20.3°$ (embankment) are clearly below the initial value $\varphi = 33.3°$ adopted for medium sands (Table 2). Reaching such low values would require a drastic structural degradation of the sand skeleton, most probably related to sustained internal erosion. This observation is consistent with the 1997 event on the dam, which was attributed to long-term filtration processes [10,11], and underlines the need for continuous piezometric monitoring.

The combination of ERT prospection and FEM-based stability analysis confirms its usefulness for the periodic assessment of hydraulic earthen structures. ERT allowed the top of the cohesive layers to be traced in a non-invasive way and, in consequence, the preferential zones of a potential slip surface to be identified. It should, however, be remembered that resistivity values strongly depend on water saturation and on the silt and clay content, so the interpretation of ERT cross-sections requires supporting information from boreholes or archival documentation. In the present study, the geological cross-sections from the literature [14–18] provided such a reference.

The boundaries between the material zones used in the ZSoil models were not taken from the resistivity images alone. The top of the cohesive layer and the position of the saturated sands read from the ERT cross-sections were checked against the shallow reference boreholes made during the field reconnaissance and against the archival borehole logs and geological cross-sections [14–18]. Only the boundaries that were confirmed by at least one of these sources were transferred to the numerical model; the resistivity ranges given in Section 4 were used mainly to follow the same layers between the control points. This limits, but does not fully remove, the well-known ambiguity of the resistivity–lithology relation. A second limitation concerns the constitutive model. An elastic–perfectly plastic Mohr–Coulomb model with a steady-state groundwater table was used for all soil layers, without strain softening and without transient seepage. Such a model is sufficient for a screening of the safety reserve and for the comparison of the variants, which is the aim of this study, but it does not reproduce the progressive, time-dependent loss of strength that is expected during long-lasting internal erosion. A prediction of the actual development of a failure in the dam body would require a more advanced model, for example with strain softening or with coupled transient flow, supported by a longer series of piezometric and geodetic observations.

Implications for the Operation of the Power Plant and the Wider Electricity System

From the perspective of electric-power engineering, the results presented here go beyond a purely geotechnical case. ESP Dychów, with 88 MW of pumping–generating capacity, belongs to a limited set of fast-responding assets on the western flank of the Polish transmission system. A forced outage caused by damage to the frontal dam or to the derivation-channel embankment would remove

© 2026 by the author(s). Distributed under a Creative Commons CC BY license.

Preprints.org (www.preprints.org) | NOT PEER-REVIEWED | Posted: 20 May 2026 doi:10.20944/preprints202605.1349.v1

this capacity from the pool of grid-balancing reserves and from the black-start portfolio of the national TSO (Transmission System Operator). The historical landslide on the frontal dam destroyed communication infrastructure and affected the powerhouse [11], which shows that a single event localised in the earthen structures may translate directly into a measurable loss of energy and capacity availability. The factor of safety well above 1.50 obtained in the analyses is therefore not a purely geotechnical statement. It is also a quantitative argument for keeping Dychów in the set of dispatchable resources that stabilise frequency and voltage in the synchronous area, in particular under the growing share of variable wind and photovoltaic generation in the Polish mix [3,4,6]. The economic dimension of this conclusion is directly relevant in the context of the Polish hydropower support schemes discussed in [5]. In this sense, the presented workflow links the periodic safety reassessment of earthen hydraulic structures directly to the operational availability of pumped-storage capacity.

Transferability of the Workflow

Analogous ageing conditions characterise a large share of the European pumped-storage fleet, including plants in Germany, Austria and the Czech Republic that were commissioned in the same decades as Dychów and operate on glaciotectonically disturbed or moraine subsoils [1,2]. Many of these twentieth-century hydroelectric schemes are today discussed also as industrial-heritage assets whose operating life is approaching its original design horizon [7], which gives an additional argument for non-invasive reassessment methods. Recent Polish case studies like the Jeziorsko reservoir on the Warta river [3,4] and, more broadly, for the Polish hydropower sector [5,6] point to a similar conclusion: the resilience of hydro assets to changing operating conditions depends not only on hydrology and on turbine characteristics, but equally on the condition of their civil structures. The ERT (with GNSS localization) plus FEM approach presented here is by construction transferable – it does not rely on dedicated instrumentation of the structure and can be repeated at regular intervals with the same set of profiles, which makes it particularly suitable for operators who manage several ageing hydro structures of Class I hydraulic-engineering rank. Repeated in a fixed two-year cycle, the same set of profiles also gives a monitoring-like signal of slow changes in the structure, which is normally available only from permanent instrumentation; this is the practical advantage that makes the procedure attractive at the scale of a whole ageing fleet rather than for a single dam.

With regard to the qualitative analysis of the channel-embankment results, attention should be drawn to the potential landslide in the lower part of the slope (variant 1A). Although its "global" safety factor (F = 2.0) is high, the vicinity of the service road for heavy vehicles introduces additional dynamic loading, which – for shallow and short slip surfaces – may have a non-negligible impact on the ratio between driving and resisting forces. A more detailed, design-level analysis including a heavy road- load, in accordance with the Polish road-engineering standard, is therefore recommended as a complementary step.

Finally, the logical consistency of the parametric results should be emphasised. In variant 2A of the dam, the limit angle $\varphi = 12.3°$ corresponds to $F \approx 1$ with groundwater included in the model; in the same configuration without groundwater, F = 1.10. Similarly, in variant 2A of the embankment, the limit angle $\varphi = 17.3°$ corresponds to $F \approx 1$ with groundwater, whereas without groundwater F = 1.55. The difference between slope with and without groundwater is related to level of water table and slip surface localization. Both outcomes are in agreement with the general behaviour of non-cohesive soils, where the presence of water reduces the overall slope capacity.

8. Conclusions

On the basis of the study, the following conclusions can be drawn:

1. Despite the complex glaciotectonic history of the cohesive soil layers, both analysed structures are stable and exhibit a considerable safety reserve. The "global" safety factor equals 1.75 for the

© 2026 by the author(s). Distributed under a Creative Commons CC BY license.

Preprints.org (www.preprints.org) | NOT PEER-REVIEWED | Posted: 20 May 2026 doi:10.20944/preprints202605.1349.v1

dam and 1.80–2.10 for the channel embankment, i.e. markedly higher than the required value of 1.50.

2. The potential presence of zones of reduced strength within the range of fluctuations of the groundwater table (e.g. loosened zones or locally higher plasticity of the cohesive soils) should not endanger the equilibrium of the analysed objects. The hypothetical slip surfaces were local and involved only a minor portion of the calculation cross-sections. The depth extent of the eventual landslides ranged from a few to about ten metres, and their shape did not differ significantly from circular–cylindrical, although slide-type movements along shallower surfaces cannot be ruled out.
3. In the case of the frontal dam, a sudden and prolonged rise of the groundwater table (e.g. as a consequence of a failure of the anti-filtration protection or of the drainage system) could adversely affect the stability of the structure. For both analysed objects, a continuous piezometric monitoring, combined with control geodetic measurements and inclinometer observations, is therefore recommended.
4. For the lower, potentially more active part of the channel-embankment slope (variant 1A), a complementary analysis including a dynamic road load in accordance with the road-engineering standard is recommended. For shallow and short slip surfaces, such loading may alter the ratio between driving and resisting forces more substantially than for deep and long surfaces.
5. Electrical resistivity tomography (ERT) is becoming one of the key and increasingly widely applied geophysical methods. It constitutes an effective tool supporting both the interpretation of traditional subsoil investigations and the identification of local anomalies that may affect design solutions, operational decisions or the interpretation of monitoring data – especially for hydraulic structures. Thanks to its non-invasive character, efficiency and low cost, ERT still offers unused potential for improving the reliability of such structures, reducing maintenance costs and effectively counteracting the effects of ageing and wear, particularly of those elements that are responsible for keeping the structure in a proper technical and safety condition.

Funding: This paper was co-financed under the research grant of the Warsaw University of Technology supporting the scientific activity in the discipline of Civil Engineering, Geodesy and Transport (grant No. 30/ILGiT/2024).

Data Availability Statement: The data that support the findings of this study are available from the corresponding author upon reasonable request.

Acknowledgments: The authors thank PGE Energia Odnawialna S.A. for making the Dychów plant accessible for the Inter-University Field Camps, and the technical staff of the plant for their valuable remarks during the field reconnaissance.

Conflicts of Interest: The authors declare no conflicts of interest.

References

1. Papadakis, N.C.; Fafalakis, M.; Katsaprakakis, D. A Review of Pumped Hydro Storage Systems. *Energies* **2023**, *16*, 4516. https://doi.org/10.3390/en16114516.
2. Kougias, I.; Aggidis, G.; Avellan, F.; Deniz, S.; Lundin, U.; Moro, A.; Muntean, S.; Novara, D.; Pérez-Díaz, J.I.; Quaranta, E.; Schild, P.; Theodossiou, N. Analysis of emerging technologies in the hydropower sector. *Renew. Sustain. Energy Rev.* **2019**, *113*, 109257. https://doi.org/10.1016/j.rser.2019.109257.
3. Hämmerling, M.; Kałuża, T.; Pilarska, A.A.; Graczyk, D.; Konieczny, K. The Role of Hydropower in Climate-Resilient Energy Systems: Case Study of the Jeziorsko Reservoir (Poland). *Energies* **2026**, *19*, 1359. https://doi.org/10.3390/en19051359.
4. Nowak, B.; Andrzejak, A.; Filipiak, G.; Ptak, M.; Sojka, M. Assessment of the Impact of Flow Changes and Water Management Rules in the Dam Reservoir on Energy Generation at the Jeziorsko Hydropower Plant. *Energies* **2022**, *15*, 7695. https://doi.org/10.3390/en15207695.

© 2026 by the author(s). Distributed under a Creative Commons CC BY license.

Preprints.org (www.preprints.org) | NOT PEER-REVIEWED | Posted: 20 May 2026 doi:10.20944/preprints202605.1349.v1

5. Godyń, I.; Dubel, A. Evolution of Hydropower Support Schemes in Poland and Their Assessment Using the LCOE Method. *Energies* **2021**, *14*, 8473. https://doi.org/10.3390/en14248473.
6. Kałuża, T.; Hämmerling, M.; Zawadzki, P.; Czekała, W.; Kasperek, R.; Sojka, M.; Mokwa, M.; Ptak, M.; Szkudlarek, A.; Czechlowski, M.; Dach, J. The hydropower sector in Poland: Historical development and current status. *Renew. Sustain. Energy Rev.* **2022**, *158*, 112150. https://doi.org/10.1016/j.rser.2022.112150.
7. Kuban, N. Hydroelectric Plants and Dams as Industrial Heritage in the Context of Nature-Culture Interrelation: An Overview of Examples in Turkey. *Energies* **2021**, *14*, 1281. https://doi.org/10.3390/en14051281.
8. PN-EN 1997-1:2008; *Eurocode 7: Geotechnical Design – Part 1: General Rules*2008.
9. PN-EN 1997-2:2008; *Eurocode 7: Geotechnical Design – Part 2: Ground Investigation and Testing*; 2008.
10. Regulation of the Minister of Transport, Construction and Maritime Economy of April 25, 2012, on determining the geotechnical conditions for the foundation of structures. *Journal of Laws of Poland* 2012, item 463. (In Polish)
11. Stilger-Szydło, E. Road earth structures. *Geoinżynieria: drogi, mosty, tunele* **2009**, *2*, 16–24. (In Polish)
12. Regulation of the Minister of Environment of April 20, 2007, on the technical conditions to be met by hydraulic structures and their location. *Journal of Laws of Poland* 2007, No. 86, item 579. (In Polish)
13. Kaczmarczyk, R.; Tchórzewska, S.; Woźniak, H. Description of selected landslides from southern Poland activated after intensive rainfall in 2010. *Biul. Państ. Inst. Geol.* **2011**, *446*, 65–73. (In Polish)
14. Kraiński, A. Glaciotectonic dislocation of the Dychów – Nowogród Bobrzański area. *Zesz. Nauk. Uniw. Zielonogórskiego, Inż. Środ.* **2007**, *134*, 101–108. (In Polish)
15. *Detailed Geological Map of Poland at 1:50,000, Sheet 573 (Bobrowice)*; Polish Geological Institute – National Research Institute: Warsaw, Poland, 2002. (In Polish)
16. *Hydrogeological Map of Poland – First Aquifer (Occurrence and Hydrodynamics) at 1:50,000, Sheet 573 (Bobrowice)*; Polish Geological Institute – National Research Institute: Warsaw, Poland, 2011. (In Polish)
17. *Hydrogeological Map of Poland – Main Useful Aquifer at 1:50,000, Sheet 573 (Bobrowice)*; Polish Geological Institute – National Research Institute: Warsaw, Poland, 2004. (In Polish)
18. Marks, L.; Grabowski, J.; Stępień, U. *Geological Map of Poland at 1:500,000*; Polish Geological Institute – National Research Institute: Warsaw, Poland, 2022. (In Polish)
19. Shi, C.; Yang, W.; Chu, W.; Shen, J.; Kong, Y. Study of Anti-Sliding Stability of a Dam Foundation Based on the Fracture Flow Method with 3D Discrete Element Code. *Energies* **2017**, *10*, 1544. https://doi.org/10.3390/en10101544.
20. Griffiths, D.V.; Lane, P.A. Slope stability analysis by finite elements. *Géotechnique* **1999**, *49*, 387–403. https://doi.org/10.1680/geot.1999.49.3.387.
21. Loke, M.H.; Chambers, J.E.; Rucker, D.F.; Kuras, O.; Wilkinson, P.B. Recent developments in the direct-current geoelectrical imaging method. *J. Appl. Geophys.* **2013**, *95*, 135–156. https://doi.org/10.1016/j.jappgeo.2013.02.017.
22. Conrad, O.; Bechtel, B.; Bock, M.; Dietrich, H.; Fischer, E.; Gerlitz, L.; Wehberg, J.; Wichmann, V.; Böhner, J. System for Automated Geoscientific Analyses (SAGA) v. 2.1.4. *Geosci. Model Dev.* **2015**, *8*, 1991–2007. https://doi.org/10.5194/gmd-8-1991-2015.
23. PN-81/B-03020; *Building Soils – Foundation Bases – Static Calculation and Design*; Polish Committee for Standardization: Warsaw, Poland, 1981. (In Polish)
24. Kaczyński, R.R. *Geological and Engineering Conditions in Poland*; Polish Geological Institute – National Research Institute: Warsaw, Poland, 2017. (In Polish)

Disclaimer/Publisher's Note: The statements, opinions and data contained in all publications are solely those of the individual author(s) and contributor(s) and not of MDPI and/or the editor(s). MDPI and/or the editor(s) disclaim responsibility for any injury to people or property resulting from any ideas, methods, instructions or products referred to in the content.

© 2026 by the author(s). Distributed under a Creative Commons CC BY license.